QSAR Analysis of 2,3Diaryl Benzopyrans/Pyrans as Selective COX2 Inhibitors Based on Semiempirical AM1 Calculations

ARTICLE *in* QSAR & COMBINATORIAL SCIENCE · OCTOBER 2004

Impact Factor: 1.55 · DOI: 10.1002/qsar.200430887

2 AUTHORS:

Sarita Prasanna
New York University
25 PUBLICATIONS **172** CITATIONS
SEE PROFILE

Manivannan Elangovan
Devi Ahilya University, Indore
27 PUBLICATIONS **182** CITATIONS
SEE PROFILE

QSAR & Combinatorial Science

QSAR Analysis of 2,3-Diaryl Benzopyrans/Pyrans as Selective COX-2 Inhibitors Based on Semiempirical AM1 Calculations

Sivaprakasam Prasanna*[1,2], Elangovan Manivannan[1] and Subash Chandra Chaturvedi[1]

Full Paper

Quantitative structure-activity relationship (QSAR) analysis was performed on a combined series of 2,3 diaryl benzopyrans and pyrans for their cyclooxygenase-2 (COX-2) inhibition. QSAR investigations based on semiempirical, Austin Model-1 (AM1) calculations reveal that electronic and hydophobic interactions are primarily responsible for COX-2 enzyme-ligand interaction. The derived QSAR model aided by residual analysis demonstrated that the COX-2 inhibitory activity is highly correlated with the electronic descriptors, lowest unoccupied molecular orbital (E_{LUMO}), Dipole-Z and hydrophobicity of the molecules. The conclusion can be drawn that more hydrophobic, electron-withdrawing substituents at 3rd aromatic ring of the lead structure improves activity. The lesser the Z component the ligand has, the more correct its orientation towards the COX-2 binding site. The derived QSAR model shows good internal (exemplified through leave one out-$q^2 = 0.786$) and external ($r^2_{pred} = 0.5737$) predictive ability for a test set and can be used in designing better selective COX-2 inhibitors among these congeners in future.

1 Introduction

Non steroidal anti-inflammatory drugs (NSAIDs) still remain among the most profusely acclaimed drugs world wide and have been prescribed in the treatment of inflammatory diseases like rheumatoid arthritis, osteo arthritis, orthopedic injuries, post operative pain, acute mylagias etc [1, 2]. The use of conventional NSAIDs has been restricted due to their adverse effects especially gastro intestinal toxicity concomitant to their therapeutic benefits. The identification of two COX enzymes has been a tremendous advance in understanding the role of prostaglandins in inflammation and the therapeutic action of NSAIDs [3]. COX-1 is constitutively expressed and is responsible for several physiological functions, whereas COX-2 is an inducible isoenzyme involved in inflammation. The beneficial anti-inflammatory effect and analgesic activities are based on the inhibition of COX-2, but the gastrointestinal toxicity and the other side effects are a result of concurrent inhibition of COX-1. The new hypothesis: inhibition of cyclooxygenase-1 (COX-1) accounts for the side effects whilst inhibition of cyclooxygenase-2 (COX-2) accounts for the therapeutic benefits of NSAIDs, opened up a rationale for the design and development of novel class of selective COX-2 inhibitors. Greater deal of attention has been paid to the diaryl heterocyclic analogues as selective COX-2 inhibitors ever since the discovery of Celecoxib and Rofecoxib. X-ray crystallographic studies [4] suggest that it is a single amino acid difference that is primarily responsible for the selectivity of most selective COX-2 inhibitors: at position 523 is an isoleucine molecule in COX-1 and valine in COX-2. The amino acid valine, which is smaller than isoleucine by a single methyl group in COX-2, allows access to a side pocket, the binding site of most selective COX-2 inhibitors, whereas the bulkier isoleucine in COX-1 blocks access to that side pocket [5].

Compounds with a central heterocyclic or carbocyclic core bearing two vicinal aryl rings have been studied in a greater extent for selective COX-2 inhibition. Substitution of one of the aromatic rings with a sulphonamido or methyl sulphonyl group is crucial for selective COX-2 inhibition. The central heterocyclic core is essential in properly orienting the aromatic rings in the COX binding site. The common heterocycles used as the central core includes pyrrole, thiazole, oxazole, furan, imidazole, isooxazole, pyrimidine, thiophene and so on. Since the last decade several selective COX-2 inhibitors have been developed and plethora of molecular modeling studies including QSAR investigations have been reported worldwide. A recent

* To receive all correspondence: [1] School of Pharmacy, Devi Ahilya Vishwavidyalaya, Ring Road, Indore-452017, India, e-mail: prasu05@rediffmail.com; [2] Present Address: Department of Medicinal Chemistry, School of Pharmacy, 417 Faser Hall, University, Mississippi, 38677, USA

Key words: AM1, COX-1, COX-2, LUMO energy, QSAR

QSAR review [6] reported by Garg et al. provides plentiful information regarding the most of the important classes of COX inhibitors. Y. H. Joo et al., introduced 2,3 diaryl benzopyran lead structure for the first time as a part of the diaryl heterocyclic family of selective COX-2 inhibitors [7]. Recently the same research group reported a novel series of 2,3 diaryl pyrans as selective COX-2 inhibitors [8]. In spite of this spectacular and unprecedented rate of progress in this therapeutic area, no molecular modeling-QSAR studies have been reported for these new lead structures. Recently we reported [9] the QSAR investigations of 2,3 diaryl benzopyrans for the first time ever since the discovery of this novel lead molecule. Owing to our special interest and in continuation of our research effort towards this lead molecule, we attempt to subject these two combined series of molecules for an effective QSAR analysis.

2 Experimental

All the computational works were performed on Pentium IV PC using ChemOffice 2001 molecular modeling software, version 6.0 supplied by Cambridge Soft Corporation, USA. COX-2 inhibitory activity data (IC_{50} in μg/ml) reported by Y. H. Joo et al., for both the series of compounds were converted to negative logarithm (pIC_{50}) in terms of molar units. IC_{50} represents the drug concentration that inhibits 50% of the COX-2 enzyme. All the activities

Table 1. Structures of 2,3 diaryl Benzopyrans/Pyrans and their COX-2 inhibitory activity

Compounds 1-26

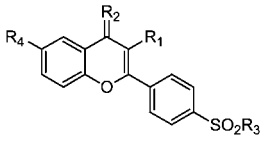

Compounds 27-44

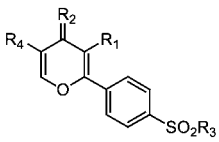

No	Substitution				pIC_{50}	No	Substitution				pIC_{50}
	R_1	R_2	R_3	R_4			R_1	R_2	R_3	R_4	
1	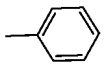	O	CH_3	H	3.0316	9	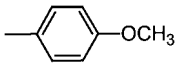	O	CH_3	H	3.2868
2*	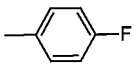	O	CH_3	H	3.6929	10	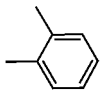	O	CH_3	H	3.0234
3#	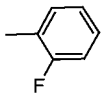	O	CH_3	H	4.1188	11#	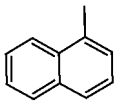	O	CH_3	H	2.4204
4	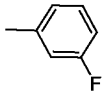	O	CH_3	H	3.2737	12*	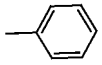	S	CH_3	H	3.9918
5*	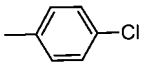	O	CH_3	H	3.4676	13	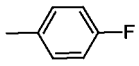	S	CH_3	H	4.1362
6	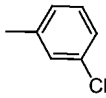	O	CH_3	H	3.4376	14	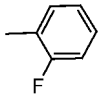	S	CH_3	H	3.7102
7*	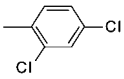	O	CH_3	H	3.4445	15#	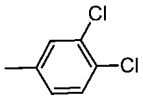	S	CH_3	H	3.2838
8	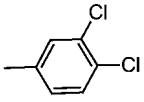	O	CH_3	H	3.5695	16*	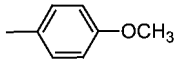	S	CH_3	H	3.8477

Table 1. (cont.)

No	Substitution				pIC_{50}	No	Substitution				pIC_{50}
	R_1	R_2	R_3	R_4			R_1	R_2	R_3	R_4	
17	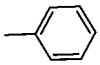	O	NH_2	H	3.9747	31	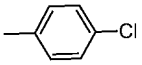	O	CH_3	Cl	3.0287;
18	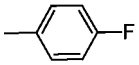	O	NH_2	H	3.8981	32*	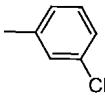	O	CH_3	Cl	2.8487
19*	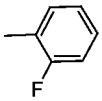	O	NH_2	H	3.7519	33	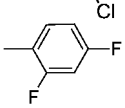	O	CH_3	Cl	2.8582
20	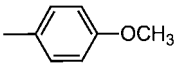	O	NH_2	H	3.4059	34	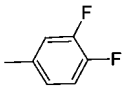	O	CH_3	Cl	2.9084
21	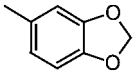	O	NH_2	H	3.0336	35*		O	CH_3	Cl	2.6301
22		O	CH_3	H	2.8778	36#	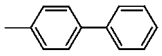	O	CH_3	Cl	4.0383
23	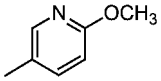	O	CH_3	H	2.6369	37	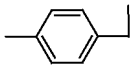	O	CH_3	Cl	3.1426
24*		O	CH_3	F	2.8981	38	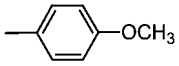	O	CH_3	Cl	2.1630
25	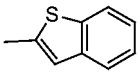	O	CH_3	H	3.4899	39*		O	CH_3	Cl	3.1331
26	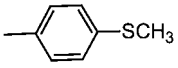	O	NH_2	H	3.5477	40	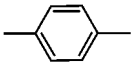	O	CH_3	Cl	2.7543
27	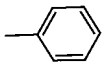	O	CH_3	Cl	2.9662	41*	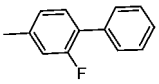	O	CH_3	Cl	4.0559
28	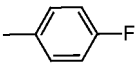	O	CH_3	Cl	2.8302	42	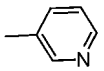	O	CH_3	Cl	2.1519
29	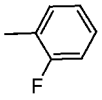	O	CH_3	Cl	2.2000	43	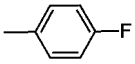	O	CH_3	H	2.6505
30*	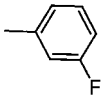	O	CH_3	Cl	2.8460	44	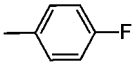	S	CH_3	Cl	3.0779

* – test set compounds.
\# – data points omitted as outliers.

retained for the study were obtained from the same biological method of evaluation using mouse peritoneal macrophages [10]. The structures and the biological activity data are given in Table 1. The molecules were sketched using Chem Draw Ultra version 6.0, cleaned copied and pasted into Chem3D ultra version 6.0. The resulting three-dimensional (3D) structures were subjected to energy minimization process using semiempirical quantum mechanics module implemented on molecular orbital package (MOPAC) version. Austin Model-1 (AM1) Hamiltonian method, closed shell restricted wave function was adopted for the energy minimization process. Dipole moment, electronic energy, HOMO energy, LUMO energy, repulsion energy and total energy (the sum of MOPAC electronic energy and the MOPAC repulsion energy) were calculated from MOPAC server of chem 3D. Since the virtual molecular orbitals are not well reproduced by Hartree-Fock methods, the HOMO and LUMO energies were calculated using AM1 method. In order to cover a wide range of physicochemical properties to describe the observed activity in a better way, we calculated other physicochemical descriptors like bending energy, charge-charge energy, charge-dipole energy, dipole-dipole energy, non-1,4 van der waals energy, stretch-bend energy, torsion energy, total energy and van der Waals energy from MM2 server of chem 3D suite. Other descriptors calculated were connolly solvent accessible surface area, connolly molecular surface area, connolly solvent excluded volume, exact mass, ovality, principal moments of inertia (X, Y, Z), Log P, molar refractivity, and heat of formation. Based on the colinearity problem among the descriptors and their contribution towards the biological activity, different mono parametric and combination of descriptors were subjected to linear regressions using SYSTAT 10.2 version. Parameters having inter correlation above $|r| > 0.5$ and those are insignificant at 95% confidence interval were not considered whilst deriving QSAR models. For the sake of brevity only the values of the descriptors used in our models are listed in Table 2. The statistical quality of the models was gauged by the parameters like correlation co-efficient (r) or squared correlation coefficient (r^2), standard error of estimate (s), variance ratio (F) and student's test value (t). The Figure within the parentheses indicates the standard error of each regression coefficient and the constant. The level of significance of each regression term was assessed using t-test.

In order to validate the derived QSAR models, leave-one-out (loo) cross validation method [11] was used. Sum of squared prediction errors called predictive residual sum of squares (PRESS) statistic [12] is calculated as the sum of squares of the differences between predicted and observed values of the activity using Val_Stat software developed at Department of Pharmacy, Shri. G. S. Institute of Technology and Science, Indore. Standard deviation of prediction (Spress), the cross-validated correlation coefficient (q^2) and standard error of predictions (SDEP) [13] were calculated for each model and taken as an estimate of the internal predictivity of the models. The external predicitivity of the models was assessed using r^2_{pred}, which is defined as $r^2_{pred} = (SD\text{-}PRESS)/SD$, where SD is the sum of the squared deviations between the biological activity of the molecules in the test set and the mean biological activity of the training set molecules and PRESS is the sum of squared deviations between predicted and observed activity for every molecule in test. Model Z score (absolute difference between the values of the model and the activity field, divided by the square root of the mean square error of the data set) was taken as a measure of outlier detection. Durbin-Watson (DW) test [14, 15] was used to check for serial correlation among residuals during regression analysis.

3 Results and Discussion

Since the number of derived predictor variables is less than the number of compounds in the training set, we attempted to obtain the correlation through multiple regression analysis module using the method of least squares.

$pIC_{50} = 0.443\ (\pm 0.046)\ LogP - 0.115\ (\pm 0.024)\ Dipole\text{-}Z - 1.086\ (\pm 0.282)\ E_{LUMO} + 0.462\ (\pm 0.427)$

$n = 28,\ r = 0.919,\ r^2 = 0.844,\ s = 0.214,\ F_{(3,24)} = 43.42,\ S_{PRESS} = 0.2515,\ Q^2 = 0.786,\ SDEP = 0.2328,\ DW = 1.718.,\ p = 0.000,\ chance < 0.01.$

The above triparametric regression equation (QSAR model) describes the COX-2 inhibitory activity of 28 benzopyran/pyran analogues as a function of their hydrophobic and electronic properties. Compounds 3, 11, 15 and 36 were omitted stepwise upon deriving the above model as outliers. This is also substantiated through the higher Z scores for these compounds indicating them as possible outliers (Figure 1). The reason for the outlying behavior is not immediately apparent. The derived model explains 84.4% variance in observed activity. LogP, the calculated partition coefficient is a measure of hydrophobicity of compounds. The positive contribution of LogP confirms the hydrophobic binding site of COX-2 enzyme and necessitates more hydrophobic molecules for improved activity. The dipole

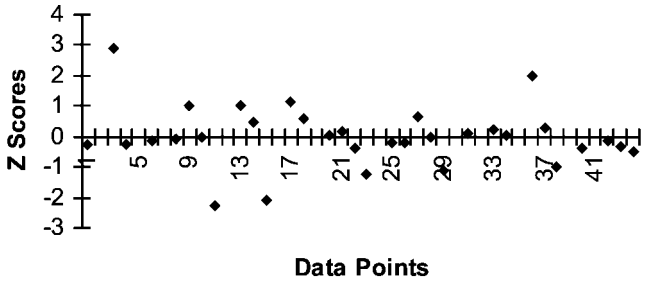

Figure 1. Z Score values of data points showing the outliers

Table 2. Descriptors and the predicted activities of molecules through derived QSAR model

Comp no	Descriptors			Predicted activity (loo)	Residual (obs-pred)
	LogP	Dipole-Z	E_{LUMO}		
1	3.32	2.322	– 1.34102	3.1259	– 0.0943
2*	3.47	2.287	– 1.44831	–	–
3#	3.47	3.809	– 1.35618	–	–
4	3.47	1.154	– 1.41371	3.4098	– 0.1361
5*	3.87	2.535	– 1.46562	–	–
6	3.87	1.380	– 1.41136	3.5610	– 0.1234
7*	4.29	2.358	– 1.30681	–	–
8	4.43	2.794	– 1.48298	3.7435	– 0.1740
9	3.19	4.211	– 1.36543	2.7975	0.4893
10	3.80	2.817	– 1.09022	2.9971	0.0263
11#	4.31	2.323	– 1.07424	–	–
12*	3.86	– 2.334	– 1.69924	–	–
13	4.02	2.187	– 1.76879	3.8159	0.3203
14	4.02	3.971	– 1.72258	3.6367	0.0735
15#	4.98	2.974	– 1.80483	–	–
16*	3.73	3.337	– 1.65801	–	–
17	3.35	– 2.605	– 1.24230	3.4987	0.4760
18	3.51	– 2.679	– 1.31948	3.7196	0.1785
19*	3.51	– 1.004	– 1.18880	–	–
20	3.23	– 1.614	– 1.23197	3.4176	– 0.0117
21	3.13	1.752	– 1.16368	2.8887	0.1449
22	2.02	– 1.307	– 1.34329	2.9847	– 0.1069
23	2.61	– 0.265	– 1.31791	3.1200	– 0.4811
24*	2.14	3.633	– 1.55843	–	–
25	4.35	2.390	– 1.39548	3.6548	– 0.1737
26	3.79	– 1.732	– 1.25252	3.7319	– 0.1842
27	1.92	2.101	– 1.44302	2.6087	0.3575
28	2.08	2.240	– 1.53303	2.7857	0.0445
29	2.08	3.972	– 1.46636	2.5558	– 0.3558
30*	2.08	3.653	– 1.57205	–	–
31	2.48	2.193	– 1.52601	2.9605	0.0682
32*	2.48	3.292	– 1.53886	–	–
33	2.24	3.676	– 1.54566	2.6939	0.1643
34	2.24	3.382	– 1.66160	2.8619	0.0465
35*	2.24	2.206	– 1.61566	–	–
36#	3.59	2.616	– 1.46805	–	–
37	2.82	2.135	– 1.42688	3.0114	0.1312
38	1.79	3.654	– 1.45006	2.4440	– 0.281
39*	1.85	2.894	– 1.44657	–	–
40	2.41	2.109	– 1.43572	2.8487	– 0.0944
41*	3.75	3.609	– 1.55884	–	–
42	0.58	3.478	– 1.56954	1.9741	0.1779
43	2.04	2.113	– 1.44741	2.6967	– 0.0462
44	2.62	2.303	– 1.78709	3.3624	– 0.2845

* – test set compounds
# – outliers for the present study

moment descriptor, Z component is a 3D electronic descriptor that indicates the strength and orientation behavior of the molecule in an electrostatic field. Dipole-Z term is attributed to the 3rd aromatic ring substitution of the lead structure. The negative correlation of the Dipole-Z term indicates that the lesser the Z component the ligand has, the more energetically favored is its correct orientation for the approach to the COX-2 binding site. This result is consistent with the most active compound 13 with 4-fluorophenyl substituion at 3rd aromatic ring. Compound 11 bearing the bulkier naphthyl ring at 3rd position of lead structure, probably due to steric effect restricts the necessary pre orientation of the entire ligand for effective interaction with the COX-2 binding site. The outlying behavior of this compound may be attributed to this steric effect. Figure 2 illustrates the energetically unfavorable orientation of compound 11, due to steric bulk at 3rd aromatic ring. Descriptor E_{LUMO} is an electronic parameter

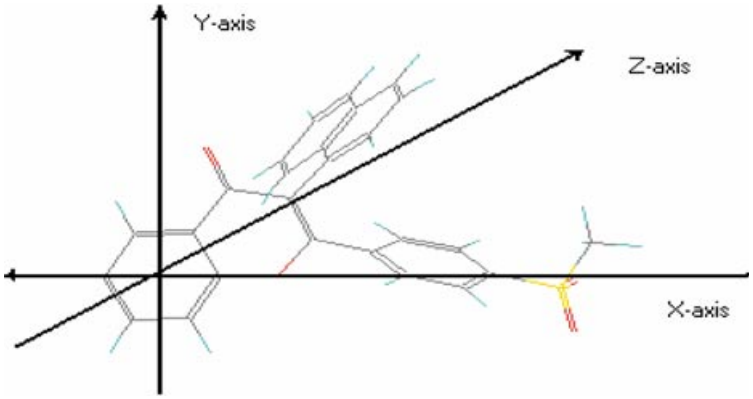

Figure 2. Positioning of the inactive member of the series in coordinate system

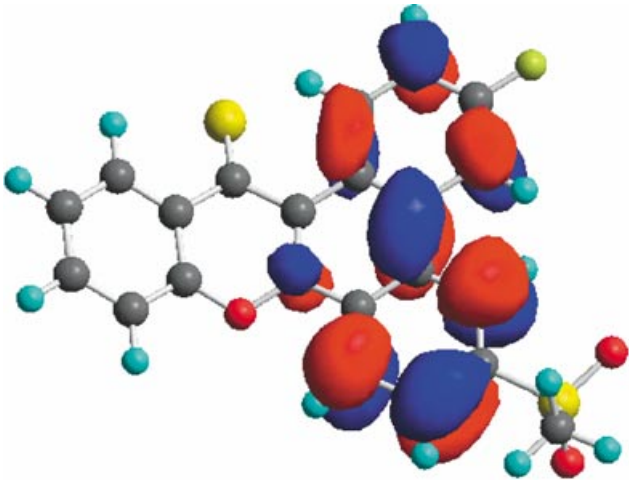

Figure 3. LUMO molecular orbitals of active member of series

and measures the electrophilicity of the molecules. When a molecule acts as a Lewis acid (an electron pair acceptor) in bond formation, incoming electrons are received in its LUMO. Molecules with low-lying LUMO are more able to accept electron than those with high energy LUMO. Figure 3 shows the LUMO orbitals of active molecule of the series. The contribution of E_{LUMO} term suggests the electron-withdrawing groups at 3rd aromatic ring of lead structure decreases the LUMO energy and in turn increases the electrophilicity of the ligands. This in turn would increase the COX-2 inhibitory activity. The fairly high variance ratio

Table 3. Inter Correlation matrix for the descriptors used in derived QSAR models

	LogP	Dipole-Z	E_{LUMO}
LogP	1.000		
Dipole-Z	0.047	1.000	
E_{LUMO}	0.040	0.252	1.000

shows the overall significance of the model. The DW statistic shows the absence of serial correlation among the residuals. All the descriptors selected for modeling COX-2 inhibitory activity are statistically significant above 99.9% confidence interval (two tailed test). The t values of 9.580, 4.820, 3.847 corroborates the statistical significance of LogP, Dipole-Z and E_{LUMO} respectively. The descriptors selected for model building are orthogonal to each other (Table 3). The derived model is ensured for its mathematical accuracy by subjecting it to residual analysis [15]. The residuals are plotted as a function of both the independent and dependent (predicted activity) variables. Figure 4a, b and c demonstrates the relationship of residuals versus the independent variables chosen for the QSAR model building. The scattering of the residuals as an approximate horizontal band rather than increasing in magnitude (Figure 4a, b, c) indicates that the residuals are independent of LogP, Dipole-Z, E_{LUMO}. This substantiates the ability of selected regression terms to model the COX-2 inhibitory activity. Figure 4d demonstrates the relationship of residuals with the predicted activities indicating the derived model as best one. The

Table 4. VIF test for multi collinearity among the descriptors for QSAR model

QSAR model	r^2	VIF
$LogP = -0.071(\pm 0.102)$ Dipole-Z $+ 0.665(\pm 1.213)$ $E_{LUMO} + 3.984$ (± 1.668)	0.059	1.063
Dipole-Z $= -0.266(\pm 0.383)$ LogP $- 5.660(\pm 2.074)$ $E_{LUMO} - 5.624$ (± 3.397)	0.266	1.362
$E_{LUMO} = 0.018(\pm 0.033)$ LogP $- 0.041(\pm 0.015)$ Dipole-Z $- 1.416$ (± 0.107)	0.261	1.353

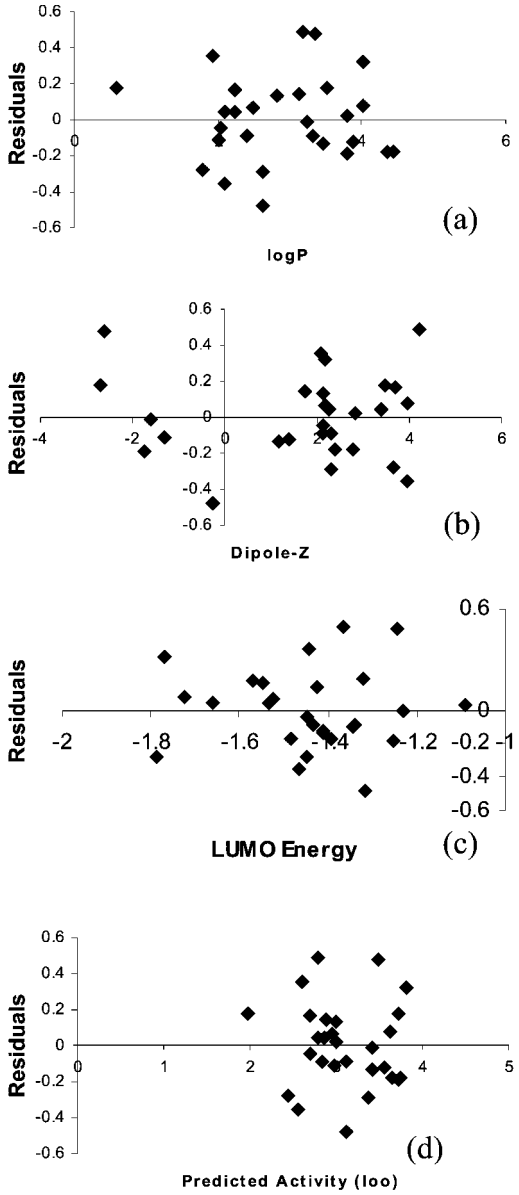

Figure 4. (a) Relationship between residuals and logP: (b) Relationship between residuals and Dipole-Z: (c) Relationship between residuals and E_{LUMO}: (d) Relationship between residuals and predicted activities through loo.

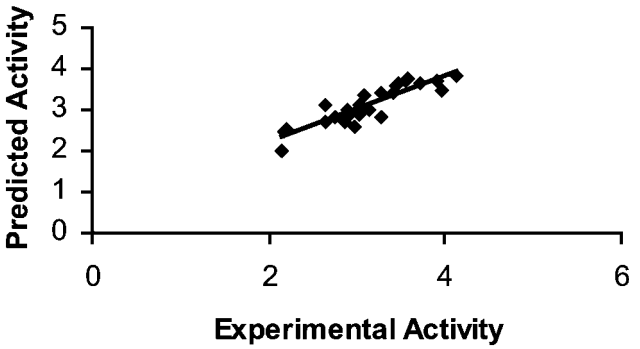

Figure 5. Experimental versus Predicted (pIC_{50}) values of training set molecules

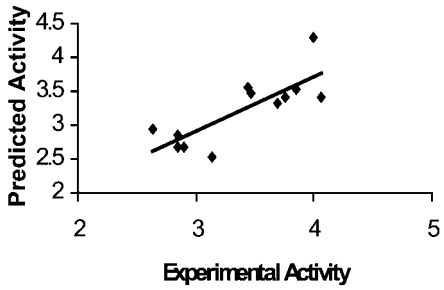

Figure 6. Experimental versus Predicted (pIC_{50}) values of test set molecules

Multicollinearity problem between the descriptors used in the derived models was tested using variance inflation data (VIF). Larger values of VIF (>10, corresponding to $r^2 > 0.9$) indicate problems with collinearity. Table 4 indicates the absence of any serious multicollinearity between the chosen descriptors. The predictive ability inside the model is good as discerned through high q^2 and less S_{PRESS} values. Since it is realized now that q^2 is no more a sufficient criterion for the predictive ability of the QSAR models, we assessed the predictive ability of our model by predicting the activity of 12 compounds externally as test set. The test set comprises of compounds 2, 5, 7, 12, 16, 19, 24, 30, 32, 35, 39 and 41 that were not included in the training set. Necessary care was ensured for the uniform distribution of biological activities among training and test set molecules. The correlation between the observed activity and the predicted activity of test set molecules was good as exemplified by $r^2_{pred} = 0.5737$. The correlation between the experimental and predicted activity for training and test set molecules is given in Figure 5 and 6.

4 Conclusion

In summary, from the derived QSAR model it can be concluded that more hydrophobic, electron-withdrawing substituents in conjugation with the 3rd aromatic ring of benzopyran/pyran lead are conducive to selective COX-2 inhibitory activity. The correlation between the LUMO energy and the COX-2 inhibitory activity clearly indicates that crucial role of charge transfer complex formation during the drug receptor interaction. The derived QSAR model validated in terms of internal and external predictive ability can aid in designing better selective COX-2 inhibitors among the congeners.

Acknowledgements

Authors S. P and E. M thank the University Grants Commission (UGC), New Delhi for the financial support for this research. Author S. P. wishes to thank Dr. S. Bharti for his constant support for this research. This research was supported by the grants from UGC, NO. F. 7-31/2003 (SR).

References

[1] C. J. Smith, Y. Zhang, C. M. Koboldt, J. Muhammad, B. S. Zweiful, A. Shaffer, J. J. Talley, J. L. Masferrer, K. Seibert, P. C. Isakson, *Annu. Rev. Physiol*. **1998**, *48*, 251 – 262.
[2] J. R. Vane, Y. S. Bakhle, R. M. Botting, *Annu. Rev. Pharmacol. Toxicol*. **1998**, *38*, 97 – 120.
[3] J. R. Vane, *Nature*, **1971**, *231*, 232 – 235.
[4] R. G. Kurumbail, J. Y. Pak, D. Gildehaus, J. M. Miyashiro, A. M. Stevens, J. K. Gierse, J. J. McDonald, R. A. Stegeman, T. D. Penning, K. Seibert, P. Isaksen, W. C. Stalling, *Nature*, **1996**, *384*, 644 – 648.
[5] C. J. Hawkey, *Lancet*, **1999**, *353*, 307 – 314.
[6] R. Garg, A. Kurup, S. B. Mekapati, C. Hansch, *Chem. Rev.* **2003**, *103*, 703 – 731.
[7] Y. H. Joo, J. K. Kim, S.-H. Kang, M.-S. Noh, J.-Y. Ha, J. K. Choi, K. M. Lim, C. H. Lee, S. Chung, *Bioorg. Med. Chem. Lett*. **2003**, *13*, 413 – 417.
[8] Y. H. Joo, J. K Kim, S.-H. Kang, M.-S. Noh, J.-Y. Ha, J. K. Choi, K. M. Lim, S. Chung, *Bioorg. Med. Chem. Lett*. **2004**, *14*, 2195 – 2198.
[9] S. Prasanna, E. Manivannan, S. C. Chaturvedi, *Bioorg. Med. Chem. Lett.* **2004**, *14*, 4005 – 4011.
[10] J. A. Mitchell, P. Akarasereenont, C. Thiermann, R. J. Flower, J. R. Vane, *Proc. Natl. Acad. Sci. U.S.A*. **1993**, *90*, 11693 – 11697.
[11] H. Kubinyi, *Quant. Struct.-Act. Relat*. **1994**, *13*, 285 – 294.
[12] S. Wold, *Quant. Struct.-Act. Relat.*. **1991**, *10,* 191 – 193.
[13] G. Cruciani, M. Baroni, D. Bonelli, S. Clementi, C. Ebert, B. Skagerberg, *Quant. Struct.-Act. Relat*. **1990**, *9*, 101 – 107.
[14] J. Durbin, G. S. Watson, *Biometrika*, **1951**, *38*, 159 – 178.
[15] J. Jeng,, A. Martin, *J. Pharm. Sci*. **1985**, *74*, 1053 – 1057.

Received on June 7, 2004; Accepted on July 24, 2004